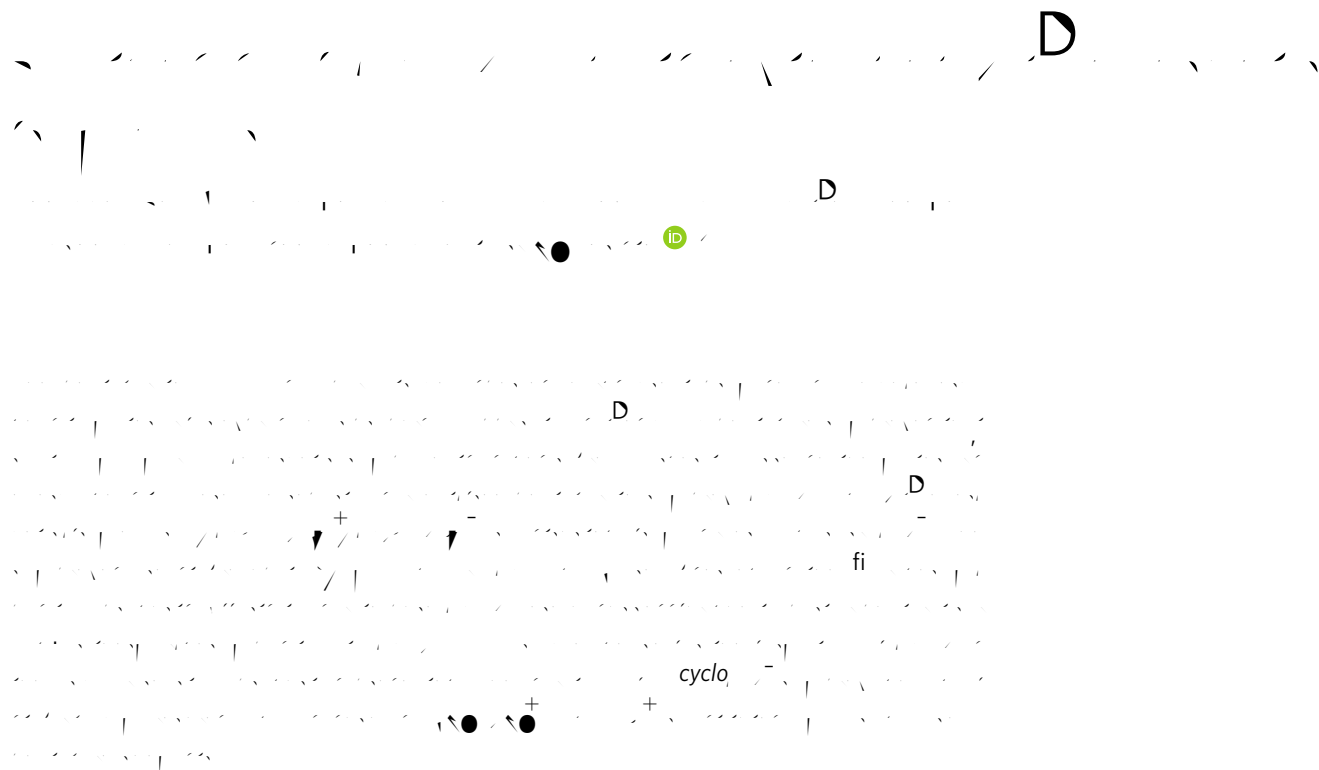


DOI: 10.1038/s41467-018-03678-y

OPEN



¹School of Chemical Engineering, Nanjing University of Science and Technology, Nanjing, Jiangsu 210094, China. ²School of Chemical Engineering, University of Science and Technology Liaoning, Anshan, Liaoning 114051, China. ³Department of Chemistry, University of Southern California, Los Angeles, CA 90089-1661, USA. These authors contributed equally: Chengguo Sun, Chong Zhang. Correspondence and requests for materials should be addressed to B.H. (email: hubb@njust.edu.cn) or to K.O.C. (email: kchriste@usc.edu)

The pentaolate anion, *cyclo*-N₅[−], has recently been stabilized as (N₅)₆(H₃O)₃(NH₄)₄Cl¹ and Co(N₅)₂(H₂O)₄ 4H₂O². This discovery has received much attention due to the potential applications of *cyclo*-N₅[−] in high-energy density materials (HEDMs) and as a starting material for the syntheses of inorganic ferrocene analogs. However, these *cyclo*-N₅[−] complexes contained non-energetic counter ions or groups to enhance their stability, thus impacting their energetic properties. The successful synthesis of an essentially naked *cyclo*-N₅[−] salt still has a huge challenge for the fascinating pentaiole chemistry and related materials science.

HEDMs require both low sensitivity and high performance³. Polynitrogen compounds hold great promise due to their fast energy release and eco-friendly decomposition products^{4–7}. Major advances in this area have been made during the past two decades, the two most remarkable new species discovered in this field are the pentaenium cation, N₅⁺,^{6–8} and the pentaiole anion, *cyclo*-N₅[−].^{9–12} However, the reported N₅⁺ and *cyclo*-N₅[−] complexes generally contain non-energetic counter ions or groups to enhance their stabilities. For example, SbF₆[−] or SnF₆^{2−} are non-energetic counter ions in N₅⁺ salts^{13,14}, and H₂O, Cl[−], NH₄⁺, and H₃O⁺ are used to stabilize the *cyclo*-N₅[−] anion¹. These non-energetic components impact their energetic properties, such as heat of formation and detonation parameters. Therefore, it is important to reduce or eliminate these non-energetic components.

As part of our long-continued research, here, we report the synthesis of a water-stabilized *cyclo*-N₅[−] salt, [Mg(H₂O)₆]²⁺[(N₅)₂(H₂O)₄]^{2−}, in which the non-energetic Cl[−] of

(N₅)₆(H₃O)₃(NH₄)₄Cl was removed. For the elimination of the water, a silver *cyclo*-N₅ complex (AgN₅) was precipitated by the addition of AgNO₃ to the [Mg(H₂O)₆]²⁺[(N₅)₂(H₂O)₄]^{2−} solution. By treatment with NH₃·H₂O, this AgN₅ complex was converted to a 3D-framework [Ag(NH₃)₂]⁺[Ag₃(N₅)₄][−] salt, which was characterized by its crystal structure. The AgN₅ complex is stable up to 90 °C, is photolytically unstable decomposing to AgN₃ and N₂, and Ag and N₂ are its only final decomposition products. The isolation of a silver *cyclo*-N₅ complex, devoid of stabilizing molecules and ions, such as H₂O, H₃O⁺, and NH₄⁺, constitutes a major advance in pentaiole chemistry.

Results

Materials synthesis and structural design. The schematic in Fig. 1 illustrates the procedures for the syntheses of the AgN₅ and [Ag(NH₃)₂]⁺[Ag₃(N₅)₄][−]. In view of previous research, our team have achieved a breakthrough in *cyclo*-N₅[−] chemistry involving the synthesis and characterization of the stable pentaiole salt, (N₅)₆(H₃O)₃(NH₄)₄Cl¹. We also demonstrated that a cobalt ion can effectively trap *cyclo*-N₅[−], forming the stable compound Co(N₅)₂(H₂O)₄ 4H₂O². As part of our continuing effort to prepare an essentially naked *cyclo*-N₅[−] salt, we first added magnesium nitrate to an aqueous solution of (N₅)₆(H₃O)₃(NH₄)₄Cl at room temperature, resulting in the formation of a white crystalline precipitate of [Mg(H₂O)₆]²⁺[(N₅)₂(H₂O)₄]^{2−} (Fig. 2) in 85% yield based on the *cyclo*-N₅[−] content of (N₅)₆(H₃O)₃(NH₄)₄Cl. Subsequently, an aqueous solution of silver nitrate was added dropwise to the stirred [Mg(H₂O)₆]²⁺[(N₅)₂(H₂O)₄]^{2−} solution in methanol, resulting in the precipitation of the AgN₅ complex as a pale

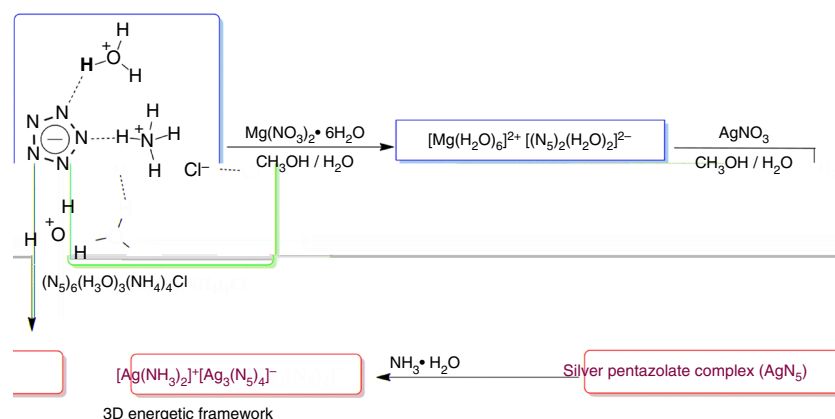


Fig. 1

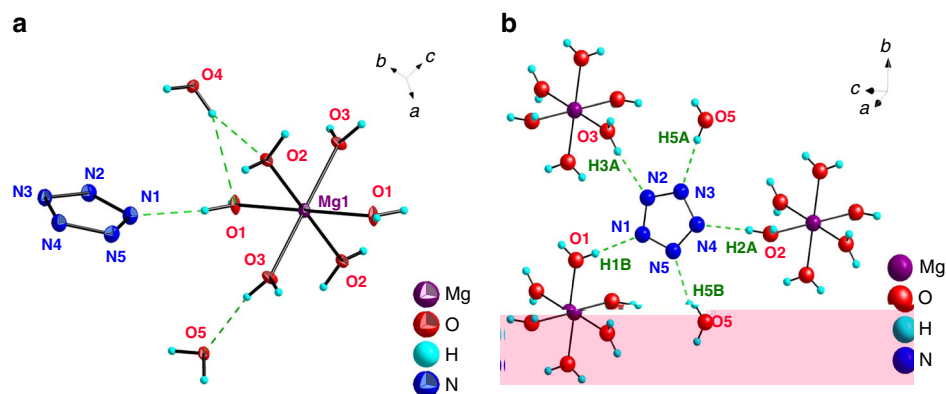


Fig. 2

white solid. However, the AgN_5 complex was light-sensitive and insoluble in all solvents tested. To further characterize this complex, we instantly treated it with 10 equiv. of $\text{NH}_3 \cdot \text{H}_2\text{O}$ (25 wt %) at 0 °C, followed by warming to room temperature to liberate NH_3 and to provide colorless crystals of $[\text{Ag}(\text{NH}_3)_2]^+[\text{Ag}_3\text{N}_5]^-$.

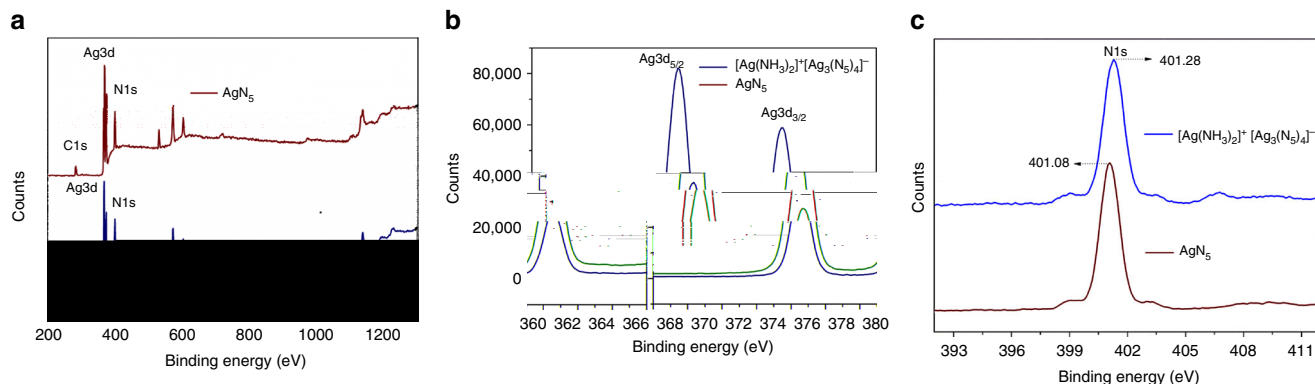


Fig. 4

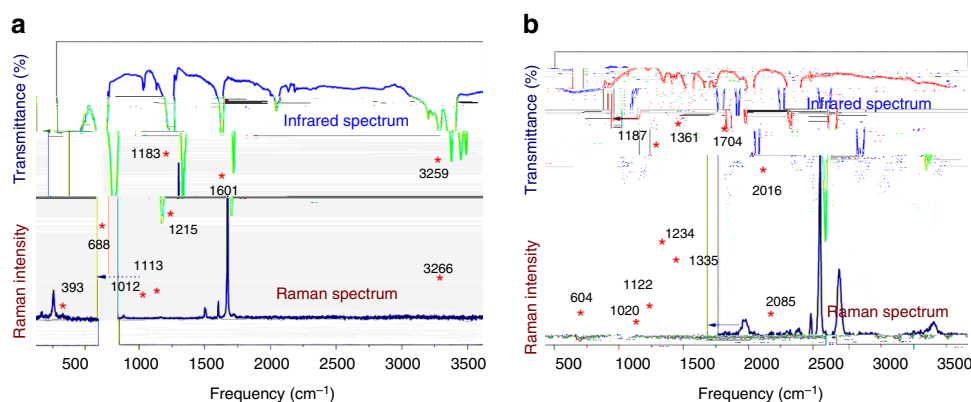


Fig. 5

Energetic metal-organic frameworks (energetic-MOFs) have recently received attention as insensitive HEDMs. The energetic-MOFs are constructed by metal ions and organic ligands, such as azides, furazans, triazoles, and tetrazoles, via coordination bonds, which give one-dimensional (1D), two-dimensional (2D) or three-dimensional (3D) structures^{17–20}. Especially noteworthy is the fact that 3D frameworks usually possess more complicated connection modes than 1D and 2D frameworks, which could further enhance their structural stability²¹. As illustrated in Fig. 3c, the silver bridged pentaolate anion in $[\text{Ag}(\text{NH}_3)_2]^+[\text{Ag}_3(\text{N}_5)_4]^-$ can also be interpreted as a 3D energetic-framework, which is constructed from Ag1, Ag2 and *cyclo*- N_5^- . The overall architecture of $[\text{Ag}(\text{NH}_3)_2]^+[\text{Ag}_3(\text{N}_5)_4]^-$ is produced with tandem coordination bonding interactions between Ag^+ and *cyclo*- N_5^- . Continuous catenation in 3D directions is made possible by independent Ag^+ centers as nodes, coordinatively bound to *cyclo*- N_5^- linkers. The propagation of both six-coordinated Ag1 and four-coordinated Ag2 to *cyclo*- N_5^- generates 3D polycatenated framework (Fig. 3f). Although Ag3 does not connect to the 3D framework, the coordinated $[\text{Ag}(\text{NH}_3)_2]^+$ is located right in the center of the voids of the crystal structure, and forms hydrogen bonds with the 3D-network (Fig. 3d), (N(11)-H(11A) N(2), 2.50 ; N(11)-H(11A) N(8), 2.31 ; N(11)-H(11B) N(5), 2.27 ; N(11)-H(11C) N(3), 2.69 ; N(11)-H(11C) N(10), 2.44). To better understand its structure, the 3D framework of $[\text{Ag}(\text{NH}_3)_2]^+[\text{Ag}_3(\text{N}_5)_4]^-$ can be topologically defined as a 3,4,4,6-c net with long Schlfli symbol of $(4\cdot6^2)_2(4^2\cdot6^3\cdot8)_2(4^3\cdot6^3)_2(4^4\cdot6^2\cdot8^6\cdot10^3)$. As shown in

Supplementary Fig. 2, topological analysis indicates that the 3D framework of $[\text{Ag}(\text{NH}_3)_2]^+[\text{Ag}_3(\text{N}_5)_4]^-$ can be abstracted as a binodal three- and four-connected net, each silver linker connects three or four *cyclo*- N_5^- anions, which corresponds better to the arrangement of atoms in the 3D framework structure. In addition, typical π - π stacking interactions are observed in $[\text{Ag}(\text{NH}_3)_2]^+[\text{Ag}_3(\text{N}_5)_4]^-$ between the two off-center parallel *cyclo*- N_5^- rings (Fig. 3e), with centroid-centroid distances of 3.634(5) and 3.838(5), respectively, which are consistent with previously reported π - π stacking distances between aromatic molecules²². The remarkable face-to-face π - π interactions are important contacts, similar to hydrogen bonding, enhancing the stability of the whole $[\text{Ag}(\text{NH}_3)_2]^+[\text{Ag}_3(\text{N}_5)_4]^-$ structure. Attempts to determine the surface area and porosity of the 3D framework by Brunner-Emmet-Teller (BET) measurements were unsuccessful because of the inability to completely degas the samples due to their limited thermal stability and the small sample sizes used.

Physicochemical properties. The $[\text{Ag}(\text{NH}_3)_2]^+[\text{Ag}_3(\text{N}_5)_4]^-$ 3D framework was further investigated by X-ray photoelectron spectroscopy (XPS). Figure 4a shows the XPS wide scan spectrum, which exhibits N1s and Ag3d peaks only. Two peaks at 368.58 and 374.48 eV generated by photoelectrons emitted from the Ag3d core level, can be observed (Fig. 4b), which indicate the presence of only one type of oxidation state for silver that coordinates to the nitrogen atoms in *cyclo*- N_5^- and NH_3 . Figure 4c

presents the high-resolution XPS results of N1s. Its binding energy at 401.28 eV is characteristic for the nitrogen atoms that form the *cyclo*-N₅⁻ ring. These XPS spectra also demonstrate the similarity of the AgN₅ units in both compounds.

We further analyzed the structure of the AgN₅ complex and [Ag(NH₃)₂]⁺[Ag₃(N₅)₄]⁻ by Raman and infrared spectroscopy. As can be seen from Fig. 5, the three typical *cyclo*-N₅⁻ RA bands are present at about 1180 cm⁻¹ (A₁[']), 1120 cm⁻¹ (E₂[']) and 1020 cm⁻¹ (E₂[']) in both compounds, in excellent agreement with the frequencies observed for (N₅)₆(H₃O)₃(NH₄)₄Cl¹. For the NH₃ coordinated cation in [Ag(NH₃)₂]⁺[Ag₃(N₅)₄]⁻ (Fig. 5a), two new characteristic bands are observed at 393 and 3266 cm⁻¹, which are due to the symmetric Ag-N₂ stretching mode of [NH₃-Ag-NH₃]⁺ and the NH₃ stretching modes, respectively^{23,24}. The infrared spectra of the two compounds show the characteristic absorption of the pentaiole rings at ca. 1225–10 cm⁻¹ that is generally present in pentaiole complexes. The assignments for the NH₃ bands in [Ag(NH₃)₂]⁺[Ag₃(N₅)₄]⁻ are unequivocal, including the different N-H stretching vibrations in the region of 3000–3400 cm⁻¹, the symmetric deformation around 1601 cm⁻¹, and the rocking mode around 688 cm⁻¹. These absorptions of [Ag(NH₃)₂]⁺ in [Ag(NH₃)₂]⁺[Ag₃(N₅)₄]⁻ agree with those of other diamine silver complexes, such as [Ag(NH₃)₂]NO₃ and [Ag(NH₃)₂]₂SO₄^{25,26}. In the 9.46459968198819984006.30910015174.16059876161.17790222158.74.32 the s371(r6s)-

$[\text{Ag}(\text{NH}_3)_2]^+[\text{Ag}_3(\text{N}_5)_4]^-$ residue exhibited the characteristic N_3^- peaks. An additional peak at 3320 cm^{-1} was assigned to HN_3 ²⁹, suggesting the generation of HN_3 during the first stage of the decomposition, followed by its absorption on the surface of AgN_3 . In the XRD analysis (Fig. 6h), the position and relative intensity of all diffraction peaks match well with those from a standard AgN_3 sample, further confirming the composition of the first-step residue as AgN_3 . The XRD powder pattern of the decomposition residue (Fig. 6h) is distinct from that of the original pattern of the starting material before decomposition (Supplementary Fig. 7). One major difference between these complexes and the previously reported $(\text{N}_5)_6(\text{H}_3\text{O})_3(\text{NH}_4)_4\text{Cl}$ or $\text{Co}(\text{N}_5)_2(\text{H}_2\text{O})_4 \cdot 4\text{H}_2\text{O}$ is that during the decomposition silver particles are produced along with complete release of N_2 . The final thermal-decomposition residue from $[\text{Ag}(\text{NH}_3)_2]^+[\text{Ag}_3(\text{N}_5)_4]^-$ was verified by optical microscopy as pure Ag, which has brilliant metallic luster and an irregular, faceted structure (Supplementary Fig. 8). We have further confirmed this result by using scanning electron microscopy (SEM) and energy dispersive X-ray spectrometry (EDX) to characterize the morphology and determine the chemical phases. Figure 6a indicates that the Ag formed from the thermal-decomposition process consists of multiple nano-layers. Each nano-layer is formed by silver nanoparticles (Fig. 6b), which have small crystallites as evidenced by the XRD analysis. The corresponding intensities of all diffraction peaks are weak due to the relatively low degree of crystallinity (Fig. 6d). The EDX spectrum shows that Ag is the only element detected in the selected region (Fig. 6c). The EDX mappings (Figs. 6e–g) recorded in the whole SEM image indicate that the element on the surface is Ag. By contrast, nitrogen is not observed in the sample region, suggesting the absence of nitrides on the Ag surface. The structure of the AgN_5 complex was also studied in more detail. The XPS wide scan spectrum of the AgN_5 complex showed no significant changes compared to that of $[\text{Ag}(\text{NH}_3)_2]^+[\text{Ag}_3(\text{N}_5)_4]^-$, indicating a similar chemical composition (except for hydrogen). The core-level spectra of N1s, and Ag3d are presented in the Fig. 4a. The only difference between the AgN_5 complex and $[\text{Ag}(\text{NH}_3)_2]^+[\text{Ag}_3(\text{N}_5)_4]^-$ is that the N1s core levels are centered at 401.08 and 401.28 eV, respectively, which illustrates that the presence of different types of nitrogen groups in the AgN_5 complex has resulted in a slight shift. The IR and Raman spectra (Fig. 5b) show only the characteristic peaks of *cyclo*- N_5^- and AgN_3 . To explain the formation of AgN_3 , a sample of the AgN_5 complex was exposed to light for 24 h, and then the IR spectrum was re-recorded. It was found that the AgN_5 complex is extremely sensitive to light and completely decomposes to AgN_3 , while the $[\text{Ag}(\text{NH}_3)_2]^+[\text{Ag}_3(\text{N}_5)_4]^-$ salt is photolytically less sensitive due to the stabilization effect by the 3D framework. In combination with the structure of $[\text{Ag}(\text{NH}_3)_2]^+[\text{Ag}_3(\text{N}_5)_4]^-$ and the aforementioned data, it, therefore, can be concluded that the AgN_5 complex is composed of AgN_5 and AgN_3 . This conclusion was further supported by elemental analysis. The total silver content was determined by inductively coupled plasma optical emission spectroscopy (ICP-OES). The found silver content in the AgN_5 complex was 62.3 wt%, intermediate between 60.7% (theoretical silver content in AgN_5) and 72% (theoretical silver content in AgN_3). The nitrogen content of another sample was also found to be intermediate between the theoretical values for AgN_5 and AgN_3 . Furthermore, the thermal stability and decomposition behavior of the AgN_5 complex were also compared to those of $[\text{Ag}(\text{NH}_3)_2]^+[\text{Ag}_3(\text{N}_5)_4]^-$. As shown in Supplementary Fig. 9, the TG curve also shows two decomposition stages. The first stage involves loss of N_2 from AgN_5 at 120. °C to give AgN_3 , and the second stage comprises the complete decomposition of AgN_3 at 332. °C to metallic Ag and N_2 .

Discussion

Our results demonstrate the successful syntheses of a solvent-free silver *cyclo*-pentaolate complex and $[\text{Ag}(\text{NH}_3)_2]^+[\text{Ag}_3(\text{N}_5)_4]^-$. The complexes are stable up to 90. °C and only Ag and N_2 are observed as the final decomposition products. The original product from the $[\text{Mg}(\text{H}_2\text{O})_6]^{2+}[(\text{N}_5)_2(\text{H}_2\text{O})_4]^{2-}/\text{AgNO}_3$ reaction is AgN_5 , which subsequently undergoes partial photolytical and/or thermal-decomposition to AgN_3 . Although we could not obtain a crystal structure for AgN_5 , the indirect evidence for its formation is convincing. The isolation of a *cyclo*- N_5^- metal complex, devoid of stabilizing molecules and ions, such as H_2O , H_3O^+ , and NH_4^+ , constitutes a major advance in *cyclo*-pentaolate chemistry.

Methods

General information. Caution! Solid silver azide and pentaolate are highly energetic and shock and friction sensitive. They should be handled only on a small scale with appropriate safety precautions, i.e., safety glasses, face shields, heavy leather gloves and jackets, and ear plugs.

Materials characterization. All reagents and solvents used were of analytical grade. $(\text{N}_5)_6(\text{H}_3\text{O})_3(\text{NH}_4)_4\text{Cl}$ was produced according to the methods described in the literature¹. Fourier-transform infrared spectra were recorded on a Thermo Nicolet IS10 instrument. Raman spectra were measured with a Renishaw (inVia) Raman spectrometer (785 nm excitation). TG-DSC-mass spectrometry (MS) measurements were performed on a Netzsch STA 409 PC/PG thermal analyzer at a heating rate of 5 K/min under argon atmosphere. X-ray photoelectron spectra (XPS) were carried out on a RBD upgraded PHI-5000C electron spectroscopy for chemical analysis (ESCA) system (Perkin Elmer) with Mg K α radiation ($h\nu = 1486.6\text{ eV}$). The crystalline structure was characterized by X-ray powder diffraction (XRD) with a X-ray diffractometer (D8 advance), using a monochromatized Cu target radiation source. The SEM mapping was observed under SEM (FEI verios 460).

Synthesis of $[\text{Mg}(\text{H}_2\text{O})_6]^{2+}[(\text{N}_5)_2(\text{H}_2\text{O})_4]^{2-}$. A solution of $\text{Mg}(\text{NO}_3)_2 \cdot 6\text{H}_2\text{O}$ (0.79 g, 3.08 mmol) in a mixture of solvents (20 mL) of methanol and water (v/v, 1/1) was added to a methanol solution of $(\text{N}_5)_6(\text{H}_3\text{O})_3(\text{NH}_4)_4\text{Cl}$ (0.2 g, 0.34 mmol) and stirred at 20. °C for 8 h. The collected filtrate was evaporated under vacuum to furnish a residue. The targeted compound could be recrystallized from the mixture of acetone and methanol and dried in vacuum at room temperature for 4 h to afford the product with an 85% yield of $[\text{Mg}(\text{H}_2\text{O})_6]^{2+}[(\text{N}_5)_2(\text{H}_2\text{O})_4]^{2-}$ as an air-stable white solid.

Synthesis of $[\text{Ag}(\text{NH}_3)_2]^+[\text{Ag}_3(\text{N}_5)_4]^-$. An aqueous solution of silver nitrate (0.34 g, 1.91 mmol) was added dropwise to a solution of $[\text{Mg}(\text{H}_2\text{O})_6]^{2+}[(\text{N}_5)_2(\text{H}_2\text{O})_4]^{2-}$ (0.3 g, 0.87 mmol) in methanol while stirring at 20. °C for 30 min, producing the silver pentaolate complex as a pale solid. It was quickly dissolved in 10 equiv. of NH_4OH and stirred at 0. °C for 20 min, followed by warming to room temperature to liberate NH_3 , providing the target product, $[\text{Ag}(\text{NH}_3)_2]^+[\text{Ag}_3(\text{N}_5)_4]^-$, in 80% yield as an air-stable white solid.

Data availability. The authors declare that the data supporting the findings of this study are available within the article and its Supplementary Information files. All other relevant data supporting the findings of this study are available on request. Structural data for $[\text{Ag}(\text{NH}_3)_2]^+[\text{Ag}_3(\text{N}_5)_4]^-$ and $[\text{Mg}(\text{H}_2\text{O})_6]^{2+}[(\text{N}_5)_2(\text{H}_2\text{O})_4]^{2-}$ were deposited with the Inorganic Crystal Structure Database (ICSD) under deposition numbers CSD: 433114 and 433851, respectively.

Received: 13 September 2017 Accepted: 5 March 2018

Published online: 28 March 2018

References

- Zhang, C., Sun, C. G., Hu, B. C., Yu, C. M. & Lu, M. Synthesis and characterization of the pentaolate anion *cyclo*- N_5^- in $(\text{N}_5)_6(\text{H}_3\text{O})_3(\text{NH}_4)_4\text{Cl}$. *Science* **355**, 374–376 (2017).
- Zhang, C. et al. A symmetric $\text{Co}(\text{N}_5)_2(\text{H}_2\text{O})_4 \cdot 4\text{H}_2\text{O}$ high-nitrogen compound formed by cobalt (II) cation trapping of a *cyclo*- N_5^- anion. *Angew. Chem. Int. Ed.* **56**, 4512–4514 (2017).
- Klappe, T. M. & Sabat, C. M. Bistetraoles: Nitrogen-rich, high-performing, insensitive energetic compounds. *Chem. Mater.* **20**, 3629–3637 (2008).
- Nguyen, M. T. Polynitrogen compounds: I. Structure and stability of N_4 and N_5 systems. *Coord. Chem. Rev.* **244**, 93–113 (2003).

5. Eremets, M. I., Gavriluk, A. G., Trojan, I. A., Diivenko, D. A. & Boehler, R. Single-bonded cubic form of nitrogen. *Nat. Mater.* **3**, 558–563 (2004).
6. Perera, S. A. & Bartlett, R. J. Coupled-cluster calculations of Raman intensities and their application to N_4 and N_5^- . *Chem. Phys. Lett.* **314**, 381–387 (1999).
7. Haiges, R. et al. Polyazide chemistry: The first binary group 6 azides, $Mo(N_3)_6$, $W(N_3)_6$, $[Mo(N_3)_7]^-$, and $[W(N_3)_7]^-$, and the $[NW(N_3)_4]^-$ and $[NMo(N_3)_4]^-$ ions. *Angew. Chem. Int. Ed.* **44**, 1860–1865 (2005).
8. Vij, A. et al. Polynitrogen chemistry. Synthesis, characterization, and crystal structure of surprisingly stable fluoroantimonate salts of N_5^+ . *J. Am. Chem. Soc.* **123**, 6308–6313 (2001).
9. Vij, A., Pavlovich, J. G., Wilson, W. W., Vij, V. & Christe, K. O. Experimental Detection of the pentaazacyclopentadienide (pentaazolate) anion, *cyclo*- N_5^- . *Angew. Chem. Int. Ed.* **41**, 3051–3054 (2002).
10. Steele, B. A. & Oleynik, I. I. Pentaazole and ammonium pentaazolate: Crystalline hydro-nitrogens at high pressure. *J. Phys. Chem. A*. **121**, 1808–1813 (2017).
11. Bažanov, B. et al. Detection of *cyclo*- N_5^- in THF solution. *Ang. Chem. Int. Ed.* **55**, 13233–13235 (2016).
12. Christe, K. O. Recent advances in the chemistry of N_5^+ , N_5^- and high-oxygen compounds. *Prop. Explos. Pyrotech.* **32**, 194–204 (2007).
13. Christe, K. O., Wilson, W. W., Sheehy, J. A. & Boat, J. A. N_5^+ : A novel homoleptic polynitrogen ion as a high energy density material. *Angew. Chem. Int. Ed.* **38**, 2004–2009 (1999).
14. Haiges, R., Schneider, S., Schroer, T. & Christe, K. O. High-energy-density materials: Synthesis and characterization of $N_5^+[P(N_3)_6]^-$, $N_5^+[B(N_3)_4]^-$, $N_5^+[HF_2]^- \cdot nHF$, $N_5^+[BF_4]^-$, $N_5^+[PF_6]^-$, and $N_5^+[SO_3F]^-$. *Angew. Chem. Int. Ed.* **43**, 4919–4924 (2004).
15. Qu, X. N. et al. An Ag(I) energetic metal–organic framework assembled with the energetic combination of furazan and tetrazole: Synthesis, structure and energetic performance. *Dalton. Trans.* **45**, 6968–6973 (2016).
16. Borrajo-Calleja, G. M. et al. Synthesis of silver(I) and gold(I) complexes containing enantiopure pybox ligands. First assays on the silver(I)-catalyzed asymmetric addition of alkynes to imines. *Inorg. Chem.* **55**, 8794–8807 (2016).
17. Krawiec, M. et al. Hydronium copper(II)-tris(5-nitrotetraazolate) trihydrate—a primary explosive. *Prop. Explos. Pyrotech.* **40**, 457–459 (2015).
18. Zhang, J. H., Dharavath, S., Mitchell, L. A., Parrish, D. A. & Shreeve, J. M. Energetic salts based on 3, 5-bis (dinitromethyl)-1, 2, 4-triazole monoanion and dianion: controllable preparation, characterization, and high performance. *J. Am. Chem. Soc.* **138**, 7500–7503 (2016).
19. McDonald, K. A., Seth, S. & Matiger, A. J. Coordination polymers with high energy density: An emerging class of explosives. *Cryst. Growth Des.* **15**, 5963–5972 (2015).
20. Seth, S. & Matiger, A. J. Coordination polymerization of 5, 5'-dinitro-2H, 2H '-3, 3'-bi-1, 2, 4-triazole leads to a dense explosive with high thermal stability. *Inorg. Chem.* **56**, 561–565 (2017).
21. Li, S. H. et al. 3D energetic metal-organic frameworks: Synthesis and properties of high energy materials. *Angew. Chem. Int. Ed.* **52**, 14031–14035 (2013).
22. Janiak, C. A critical account on π - π stacking in metal complexes with aromatic nitrogen-containing ligands. *J. Chem. Soc. Dalton. Trans.* **21**, 3885–3896 (2000).
23. Nilsson, K. B., Persson, I. & Kessler, V. G. Coordination chemistry of the solvated AgI and AuI ions in liquid and aqueous ammonia, trialkyl and triphenyl phosphite, and tri-n-butylphosphine solutions. *Inorg. Chem.* **45**, 6912–6921 (2006).
24. Ujike, T. & Tominaga, Y. Raman spectral analysis of liquid ammonia and aqueous solution of ammonia. *J. Raman Spectrosc.* **33**, 485–493 (2002).
25. Woidy, P. & Kraus, F. The diammine silver(I) acetate $[Ag(NH_3)_2]OAc$. *Z. Anorg. Allg. Chem.* **639**, 2643–2647 (2013).
26. Geddes, A. L. & Bottger, G. L. Infrared spectra of silver-ammine complexes. *Inorg. Chem.* **8**, 802–807 (1969).
27. Grocholl, L., Wang, J. J. & Gillan, E. G. Synthesis of sub-micron silver and silver sulfide particles via solvothermal silver azide decomposition. *Mater. Res. Bull.* **38**, 213–220 (2003).
28. Iqbal, Z., Prask, H. J. & Trevino, S. F. in *Energetic Materials* (eds Fair, H. D. & Walker, R. F.) 131–191 (Plenum Press, New York, 1977).
29. Dows, D. A. & Pimentel, G. C. Infrared spectra of gaseous and solid hydrazoic acid and deuterio-hydrazoic acid: The thermodynamic properties of HN_3 . *J. Chem. Phys.* **23**, 1258–1263 (1955).

Acknowledgements

We are grateful for financial support provided by the Fundamental Research Funds for the Central Universities (No. 30917011101), University of Science and Technology Liaoning Fund for Young Talent (No. 601011506-8), and the Priority Academic Program Development of Jiangsu Higher Education Institutions. We also thank Huaping Bai (Analysis and Testing Center of Nanjing University of Science and Technology) for testing of the XRD spectra, Wanying Tang (Analysis and Testing Center of Nanjing University of Science and Technology) for testing of the IR spectra, Wenxian Wei (Yangzhou University) for testing of the Raman spectra, Chuanqiang Zhou (Yangzhou University) for testing of the XPS spectra and Fengfeng Wang (Institute of Materia Medica, Chinese Academy of Medical Science & Peking Union Medical College) for his expert crystallographic analysis. Karl Christe gratefully acknowledges financial support from the Office of Naval Research.

Author contributions

B.H. designed the scheme and conducted experiments. C.S., C.Z., C.J., C.Y., Y.D., Z.Z., and Y.Z. conducted the experiments. All the authors contributed to discussions of the results for the manuscript. C.S. and C.Z. wrote the manuscript. B.H., C.J., and Y.D. reviewed this manuscript. K.C. gave important suggestions on the paper and discussed the characterization of the silver pentaazolate complex, he also revised this manuscript.

Additional information

Supplementary Information accompanies this paper at <https://doi.org/10.1038/s41467-018-03678-y>.

Competing interests: The authors declare no competing interests.

Reprints and permission information is available online at <http://npg.nature.com/reprintsandpermissions/>

Publisher's note: Springer Nature remains neutral with regard to jurisdictional claims in published maps and institutional affiliations.



Open Access This article is licensed under a Creative Commons Attribution 4.0 International License, which permits use, sharing, adaptation, distribution and reproduction in any medium or format, as long as you give appropriate credit to the original author(s) and the source, provide a link to the Creative Commons license, and indicate if changes were made. The images or other third party material in this article are included in the article's Creative Commons license, unless indicated otherwise in a credit line to the material. If material is not included in the article's Creative Commons license and your intended use is not permitted by statutory regulation or exceeds the permitted use, you will need to obtain permission directly from the copyright holder. To view a copy of this license, visit <http://creativecommons.org/licenses/by/4.0/>.

© The Author(s) 2018